NUS National University of Singapore | College of Design and Engineering

ME6303 Presentation:

Experimental investigation on compressible flow over a circular cylinder at 1000 ≤ Re ≤ 5000

Paper Authors: T. Nagata, A. Noguchi, K. Kusama, et al. (Tohoku University)

Presenter:
Huanxia WEI A0285164Y (Master of Science in Mechanical Engineering) &
Hao HU A0288062Y (Doctoral Student in Mechanical)
Supervisor: Danielle S. Tan

16. November 2023

Contents

Basic Information

Title: Experimental investigation on compressible flow over a circular cylinder at Reynolds number of between 1000 and 5000.

Journal: Journal of Fluid Mechanics (Area Top), 2020.

Authors: Nagata, T., Noguchi, A., Kusama, K., Nonomura, T., Komuro, A., Ando, A., and Asai, K.

Affiliation: Tohoku University

Research Background: *Objectives*

Flow over a circular cylinder is a classic and significant problem in fluid mechanics. The features of the Karman vortices and the Strouhal number of vortex shedding (St) are always be noticed.

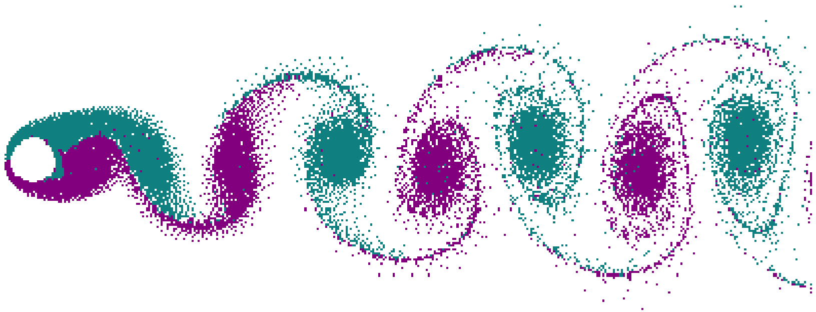

Compressible flow is defined as a type of fluid flow in which the fluid's density changes significantly as it moves. The study of compressible flow is vital in many engineering applications.

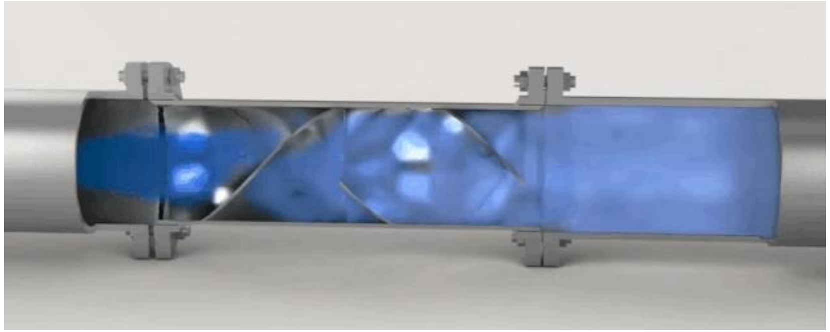

Research Background: *Related Works*

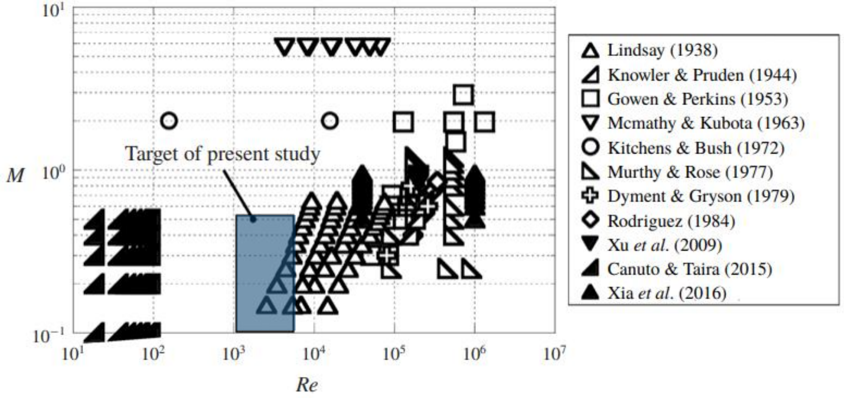

FIG: Map of the conditions investigated in the previous studies. Lindsey (1938): exp., drag measurement; Knowler & Pruden (1944): exp., drag and pressure measurement; Gowen & Perkins (1953): exp., drag and pressure measurement, **shadowgraph**; McCarthy & Kubota (1964): exp., pitot-pressure, static pressure and total temperature measurements, schlieren; Kitchens & Bush (1972): exp., hot-wire measurement, **shadowgraph**; Murthy & Rose (1977): exp., pressure and skin friction measurement; Dyment & Gryson (1979): exp., **shadowgraph and schlieren**; Rodriguez (1984): exp., **shadowgraph** and unsteady pressure measurement; Xu et al. (2009): num., DES; Canuto & Taira (2015): num., DNS; Xia et al. (2016): num., CLES.

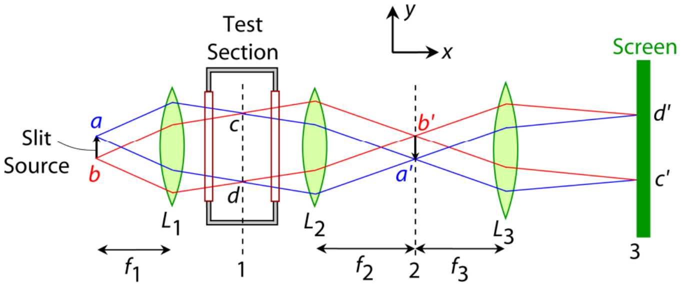

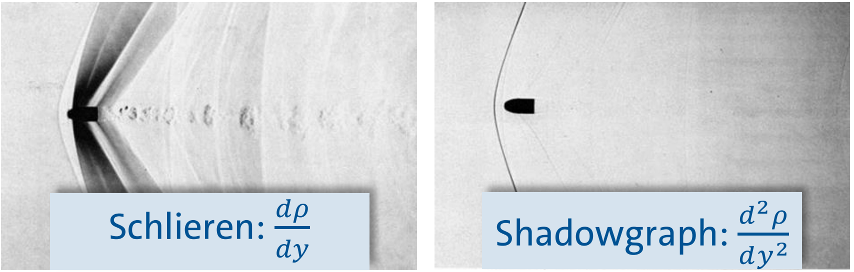

FIG: Bullet at M=1.1, from Van Dyke (1982).

Research Contents (Overview)

Conditions. subsonic (0.1-0.5 Mach), compressible, turbulence (relative low Re 1000-5000), two-dimensional, focus on steady (mainly time-averaged), small scaled, low pressure (P_0 1-50 kPa), temperature unknown, experimental methods (not CFD).

Problem. flow (air) over a circular cylinder.

Tools. low-density wind tunnel (main), schlieren, pressure-sensitive paint PSP (incl. auto spectrum for PSD and cross spectrum for phase), WT balance system.

Focus. features of karman vortices (i.e., wake structure, incl. PSD, phase, shape of wake, St.), Re and Mach vs St, Cp and Cd (magnitude and phase changes).

Experimental Setups

Mars Wind Tunnel, Tohoku-University ***(野々村·永田·佐々木研究室).*** LINK

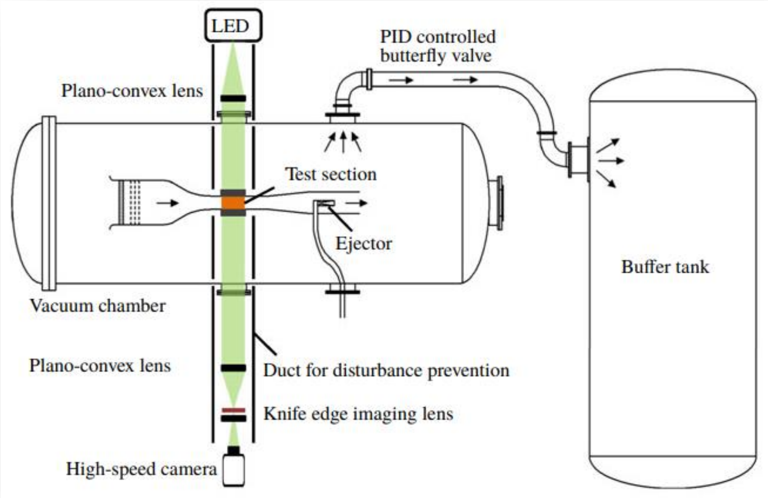

FIG: Schematic of the mars wind tunnel of Tohoku University.

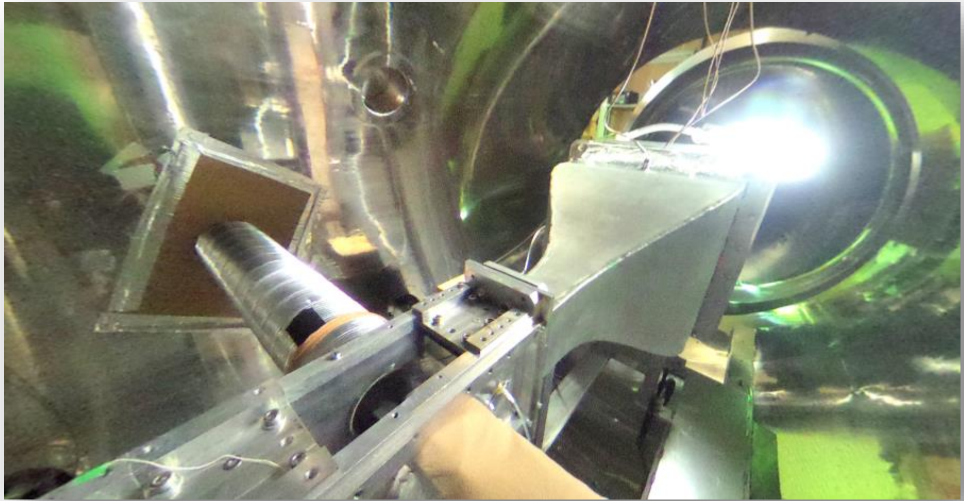

FIG: internal photo of the mars wind tunnel of Tohoku University.

Experimental Setups

Mars Wind Tunnel, Tohoku-University ***(野々村·永田·佐々木研究室).*** LINK

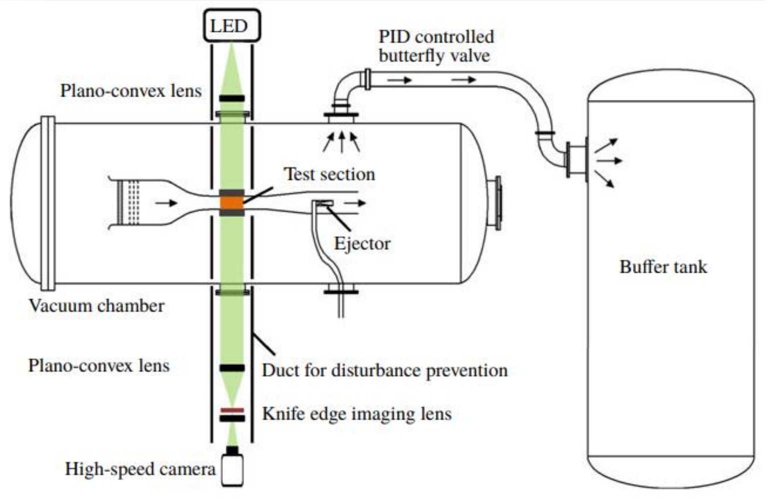

FIG: Schematic of the mars wind tunnel of Tohoku University.

Type: suction wind tunnel, subsonic, high speed (compressible low Reynolds number flow).

Test section: 150 × 100 × 600 mm rectangular section.

Mach: 0.1-0.74 mach.

Applications: simulating the flow around an aircraft flying in the Martian atmosphere and **for fundamental study on compressible low-Reynolds-number flow**.

Owner: Experimental Aerodynamics Laboratory, TohokuU.

Experimental Setups

Measuring tools in this case.

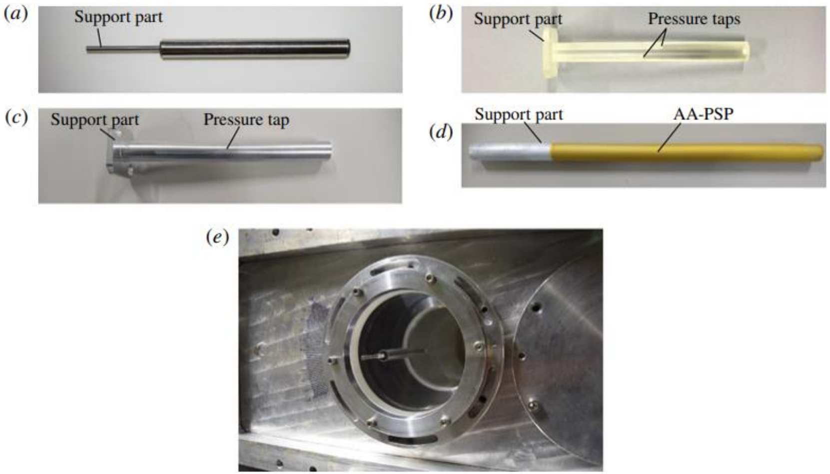

FIG: Test modes: (a) for schlieren visualization; (b) for steady pressure measurement; (c) for unsteady pressure measurement; (d) for PSP measurement (e) mounted model on the optical window (schlieren set-up).

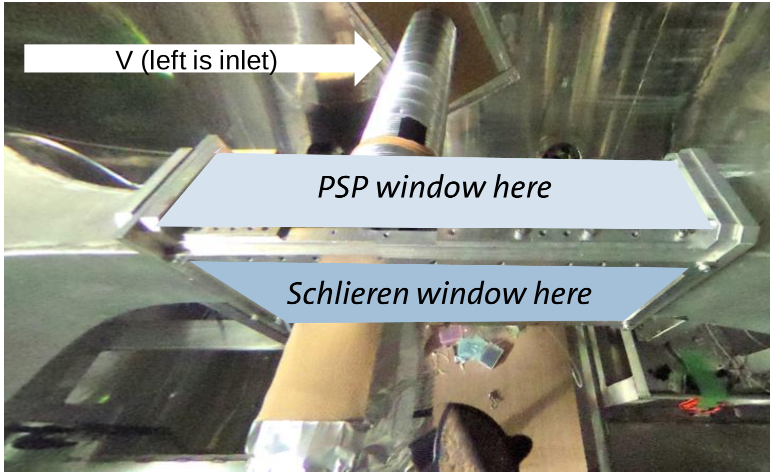

FIG: Test section of Mars wind tunnel, Tohoku University (left and right reversed).

Results and Discussion: *Instantaneous flow field*

Flow structure

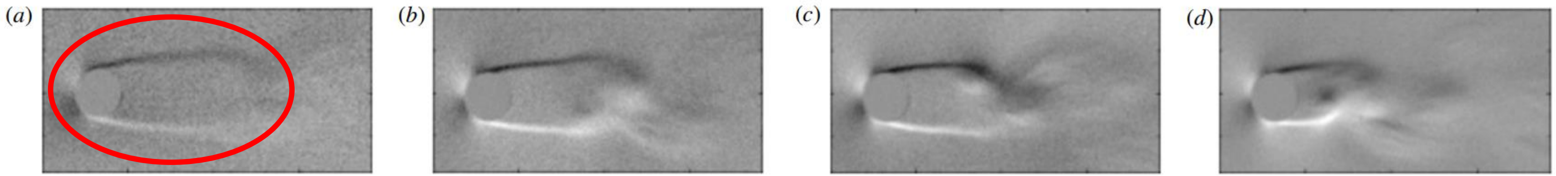

FIG: Effect of Re on the instantaneous flow field at M=0.5. (a) Re=1000; (b) Re=2000; (c) Re=3000; (d) Re=4000.

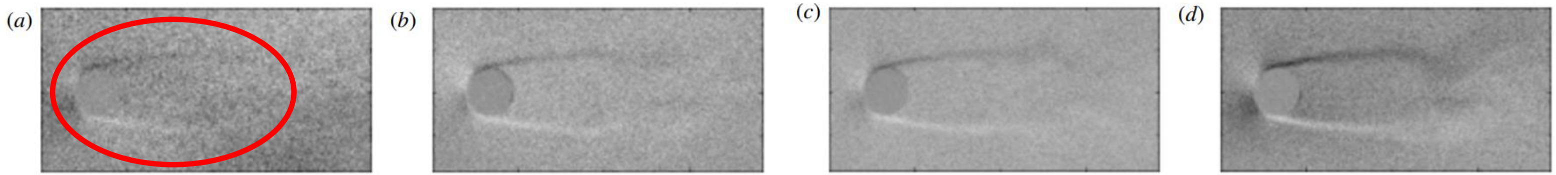

FIG: Effect of M on the instantaneous flow field at Re=1000. (a) M=0.2; (b) M=0.3; (c) M=0.4; (d) M=0:5.

- The shear layer length decreases as Re increases or M decreases.
- The images are unclear at low-Re and low-M. ⇨ Small density fluctuation ⇨ Root-mean-square (rms) density

Results and Discussion: *Instantaneous flow field*

Flow structure

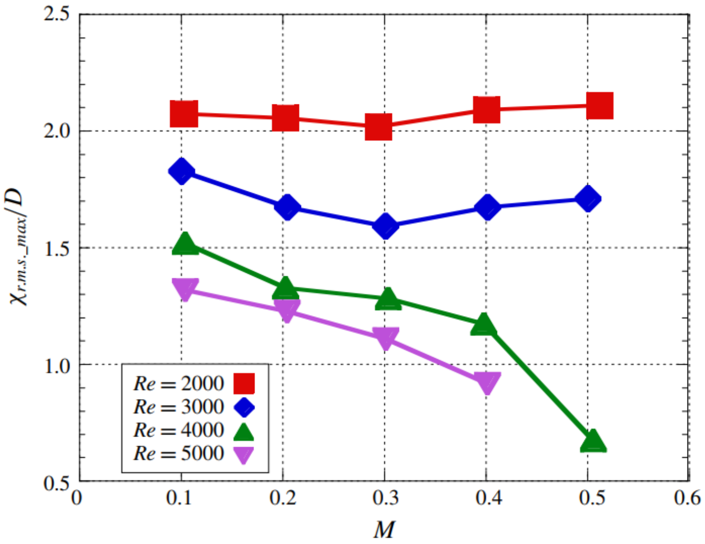

FIG: Effect of M on the position of the maximum r.m.s. of intensity of the schlieren image.

- The maximum r.m.s. position is related to the length of the recirculation region.
- The M dependence on the maximum r.m.s. point is different between Re≤3000 and Re≥4000 while M>0.3.

⇧

Kelvin–Helmholtz instability and oblique instability

Results and Discussion: *Instantaneous flow field*

Flow structure

- Kelvin–Helmholtz instability

- It occurs when there is velocity shear in a single continuous fluid or a velocity difference across the interface between two fluids.
- It can be suppressed by compressibility.

- Oblique instability

- It should be differed from the oblique shock wave.
- As Re increases, the vortex shedding becomes oblique, where the vortices are parallel to each other but inclined with respect to the cylinder axis.

Results and Discussion: *Instantaneous flow field*

Flow structure

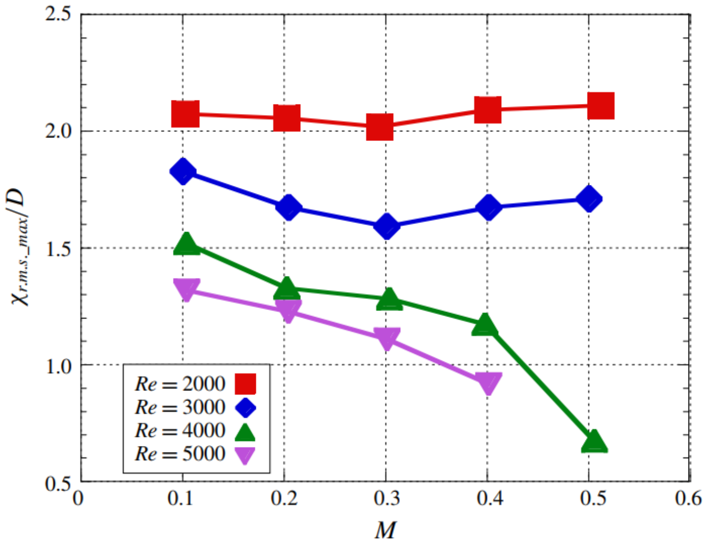

FIG: Effect of M on the position of the maximum r.m.s. of intensity of the schlieren image.

- For Re≤3000

  The Kelvin–Helmholtz instability is suppressed by compressibility.

  As M increases, the recirculation region is more stable, so the length would increase.

- For Re≥4000

  The oblique instability is dominant and surpasses the decreasing Kelvin–Helmholtz instability.

  As M increases, the recirculation region is less stable, so the length would decrease.

Results and Discussion: *Instantaneous flow field*

Planar distribution of pressure fluctuation

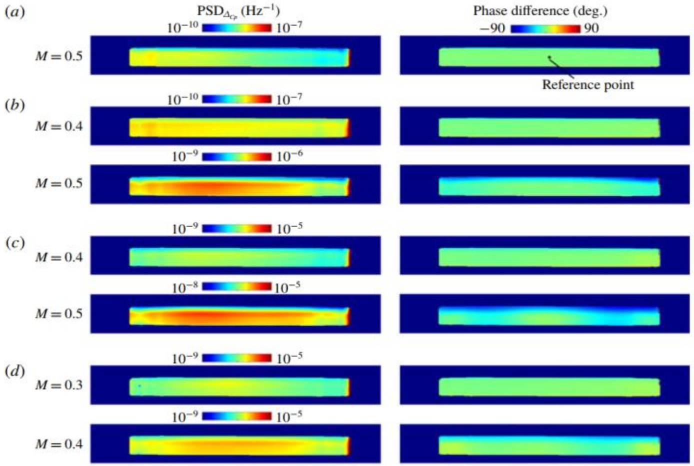

FIG: Distributions of PSD and phase difference of ΔC_p. (a) Re=2000; (b) Re=3000; (c) Re=4000; (d) Re=5000.

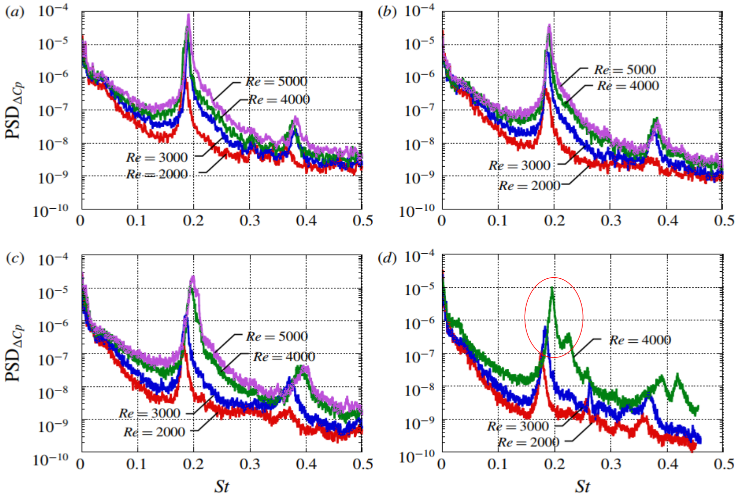

FIG: Frequency spectra of PSD. (a) M=0.2; (b) M=0.3; (c) M=0.4; (d) M=0.5.

- The pressure fluctuation and the phase difference becomes stronger at higher-Re and -M conditions.
- The competing frequency appears at Re=4000 and M=0.5.

Results and Discussion: *Instantaneous flow field*

Strouhal number of vortex shedding

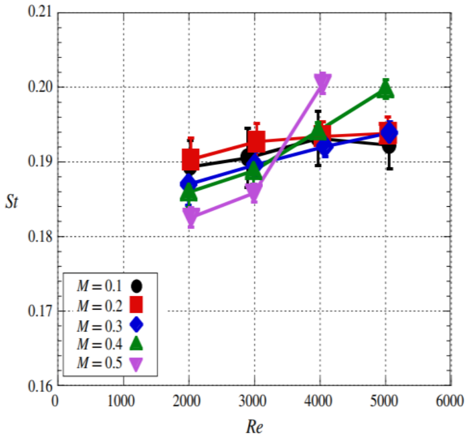

FIG: Effect of Re on St of vortex shedding.

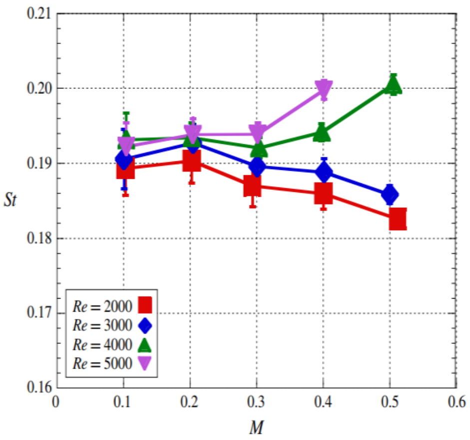

FIG: Effect of M on St of vortex shedding.

- St of vortex shedding increases as Re increases.
- For M≤0.3, St of vortex shedding is not related to M.
- For M>0.3, the M dependence on St of vortex shedding is different in Re≤3000 and Re≥4000.

Similar to the case of the flow structure

⇧

Oblique instability

Possibility of mode transition? LINK

Results and Discussion: *Time-averaged flow field*

Mean-flow field

(*a*)

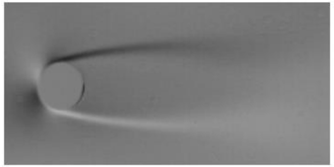

(*d*)

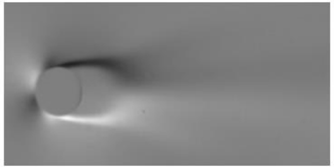

FIG: Effect o ...) Re=4000.

(*a*)

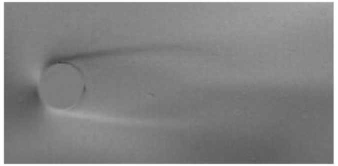

(*d*)

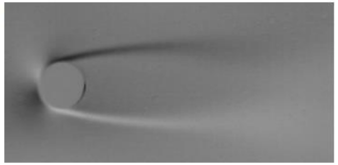

FIG: Effe ... M=0:5.

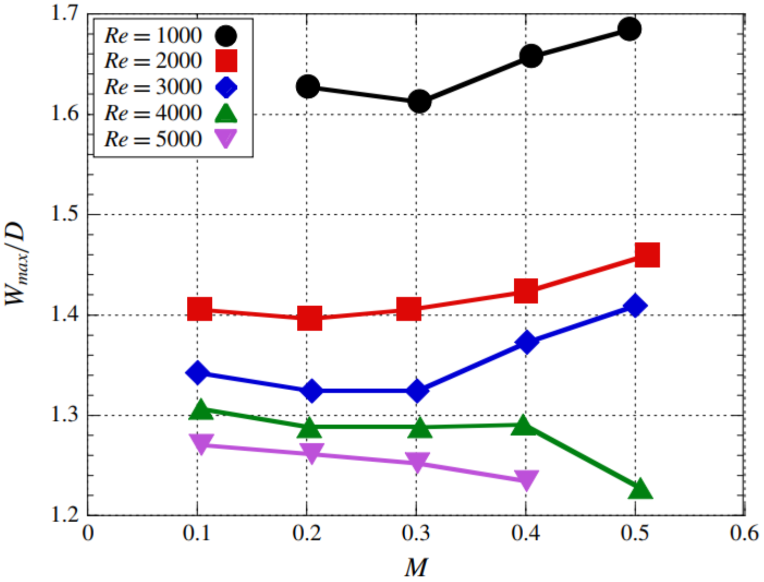

FIG: Effect of M on the maximum width of the separated shear layer.

Similar to the results of the instantaneous flow field

Results and Discussion: *Time-averaged flow field*

Distribution of pressure coefficient

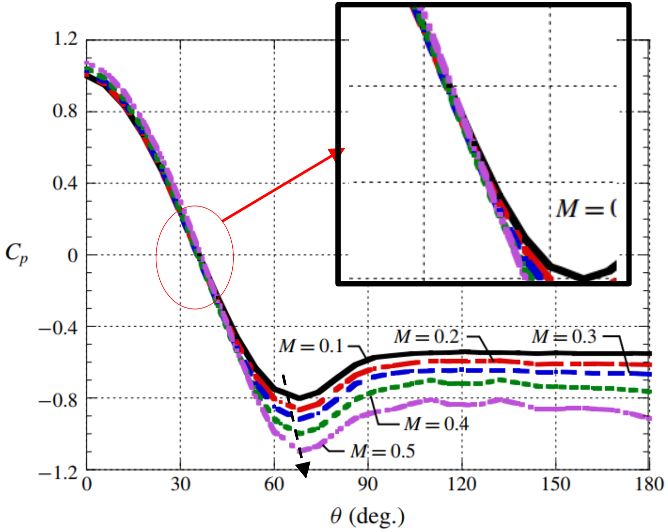

FIG: Time-averaged pressure coefficient distribution for different M (Re=4000).

- The trend of the M effect on the time-averaged pressure coefficient reverses around θ=45°.

⇧

Prandtl–Glauert transformation

A mathematical technique for solving compressible flow problems by incompressible flow calculations, which increases the absolute value of C_p as M increases.

- The position of the minimum C_P (the separation point) appears to move downstream as M increases.

⇧

The M effect on the viscous drag coefficient

Results and Discussion: *Time-averaged flow field*

Drag coefficient

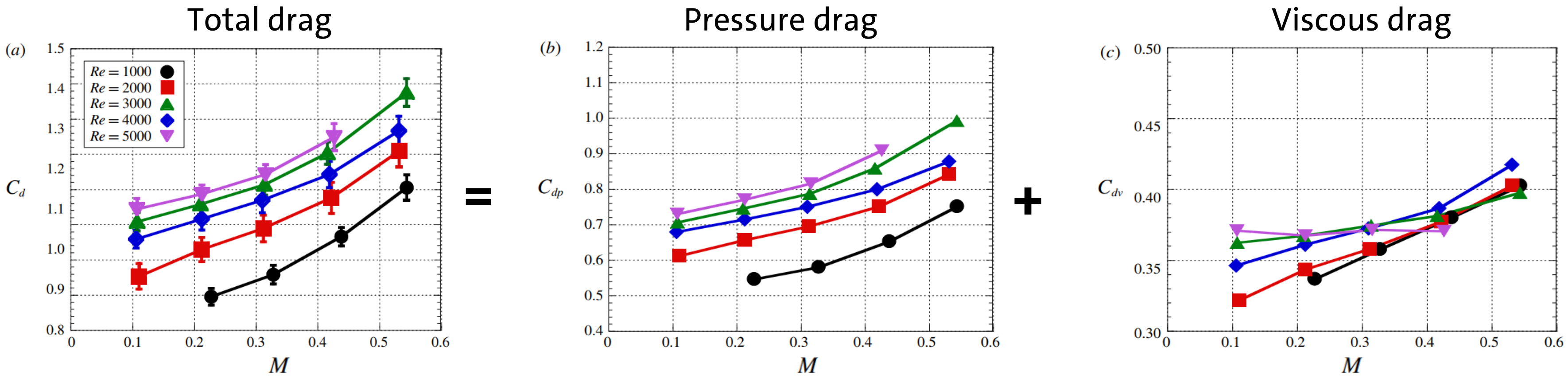

FIG: Effect M on the drag coefficient. (a) Total; (b) pressure component; (c) viscous component.

- The increment of the total drag coefficient is almost due to the increment of the pressure component, because of the Prandtl–Glauert transformation.
- The viscous component of the drag coefficient increases as *M* increases but the increment is quite small.

Conclusions

The properties of the compressible low-Re flow over a circular cylinder were experimentally investigated using the low-density wind tunnel with time-resolved schlieren visualizations and pressure and force measurements. Effects of M between 0.1 and 0.5 on the flow characteristics are clarified for Re between 1000 and 5000.

- The trend of M effect on the flow field, that are the release location of the Kármán vortices, the Strouhal number of vortex shedding and the maximum width of the recirculation, is changed at approximately Re=3000.
- The observed spanwise phase difference is considered to the oblique instability wave on the separated shear layer caused by the compressibility effects.
- The Strouhal number of the vortex shedding is influenced by M and Re, and those effects are nonlinear.

Additionally Insights

- Small dt for recording
- 2d image sequence
- Scalar field function

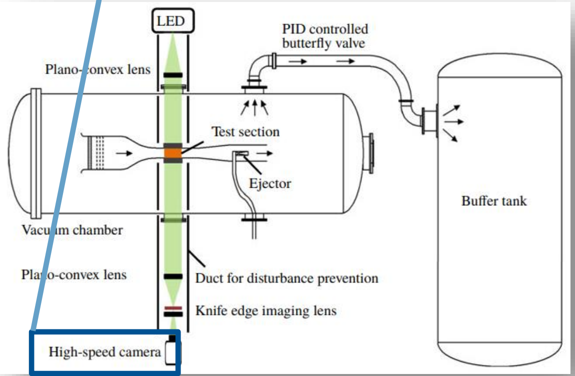

Mode Decomposition

*DMD***, *SPOD**, *POD**, ……

$$A = U\Sigma V^T \simeq \sum_{i=1}^{k} u_i \sigma_i v_i \quad , k \le r = rank(A)$$
$$D = \Phi\Sigma C^T \simeq \sum_{i=1}^{k} \phi_i \sigma_i c_i \quad , k \le r = rank(D)$$
$$v_{i+1} = A v_i$$
$$V_1^N = \{v_1, v_2, \ldots, v_N\} = \{v_1, Av_1, A^2 v_1, \ldots, A^{N-1} v_1\}$$

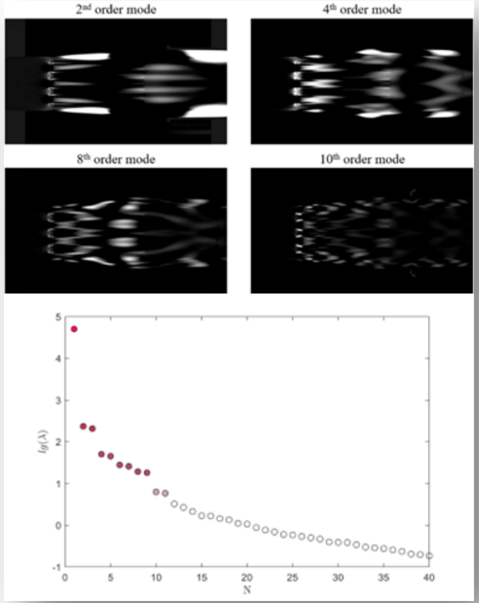

**(S)POD: (Spectral) Proper orthogonal decomposition. **DMD: Dynamic mode decomposition.*

Additionally Insights

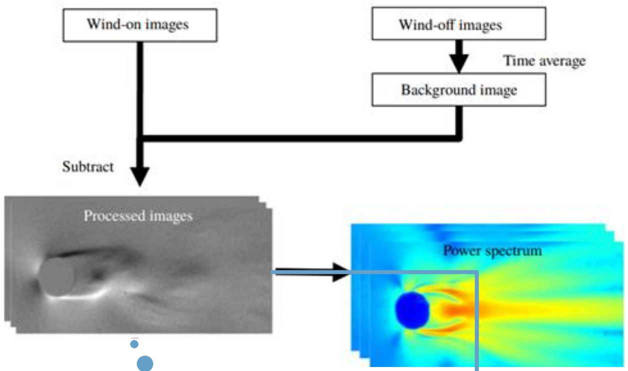

“ I am a 20000-fps TIME sequence ! ”

Mode Decomposition

DMD**

SPOD*

POD*

……

$$A = U\Sigma V^T \simeq \sum_{i=1}^{k} u_i \sigma_i v_i \quad ,k \le r = rank(A)$$

$$D = \Phi\Sigma C^T \simeq \sum_{i=1}^{k} \phi_i \sigma_i c_i \quad ,k \le r = rank(D)$$

$$v_{i+1} = Av_i$$

$$V_1^N = \{v_1, v_2, \ldots, v_N\} = \{v_1, Av_1, A^2 v_1, \ldots, A^{N-1} v_1\}$$

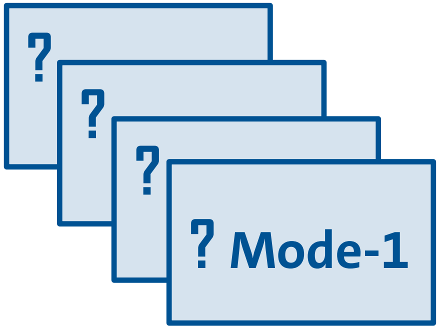

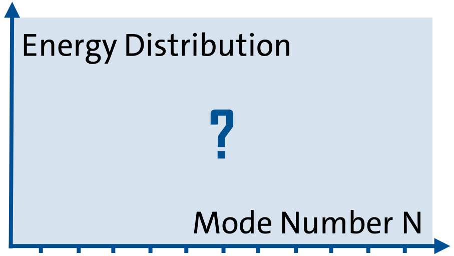

*(S)POD: (Spectral) Proper orthogonal decomposition. **DMD: Dynamic mode decomposition.

References

Wind tunnel facility (high-speed) / circular cylinder wind tunnel tests

1. **Achenbach, E., & Heinecke, E. (1981). On vortex shedding from smooth and rough cylinders in the range of Reynolds numbers 6e3 to 5e6. Journal of Fluid Mechanics, 109, 239-251. doi: 10.1017/S002211208100102X**
2. Chen, J. G., Zhou, Y., Antonia, R. A., & Zhou, T. M. (2019). The turbulent Kármán vortex. Journal of Fluid Mechanics, 871, 92-112. doi: 10.1017/jfm.2019.296
3. Greco, C. S., Paolillo, G., Astarita, T., & Cardone, G. (2020). The von Kármán street behind a circular cylinder: flow control through synthetic jet placed at the rear stagnation point. Journal of Fluid Mechanics, 901, A39, Article A39. doi: 10.1017/jfm.2020.427
4. **Jiang, H., & Cheng, L. (2017). Strouhal–Reynolds number relationship for flow past a circular cylinder. Journal of Fluid Mechanics, 832, 170-188. doi: 10.1017/jfm.2017.685**
5. Ooi, A., Chan, L., Aljubaili, D., Mamon, C., Leontini, J. S., Skvortsov, A., Mathupriya, P., & Hasini, H. (2020). Some new characteristics of the confined flow over circular cylinders at low reynolds numbers. International Journal of Heat and Fluid Flow, 86, 108741. doi: 10.1016/j.ijheatfluidflow.2020.108741
6. Zhao, M. (2021). Flow past a circular cylinder and a downstream sphere for Re=300. Journal of Fluid Mechanics, 913, A20, Article A20. doi: 10.1017/jfm.2020.1123

Schlieren, shadowgraph, PSP

7. Lakshmi, R. V., Aruna, S. T., & Basu, B. J. (2020). Luminescent Paint for Air Pressure Sensing. Resonance, 25(11), 1579-1593. doi: 10.1007/s12045-020-1076-x
8. **Prenel, J.-P., & Ambrosini, D. (2012). Flow visualization and beyond. Optics and Lasers in Engineering, 50, 1-7. doi: 10.1016/j.optlaseng.2011.10.003**
9. Sun, Z., Gan, T., & Wu, Y. (2019). Shock-Wave/Boundary-Layer Interactions at Compression Ramps Studied by High-Speed Schlieren. AIAA Journal, 58(4), 1681-1688. doi: 10.2514/1.J058257
10. Vaisakh, S., & Muruganandam, T. M. (2020). Affordable schlieren visualization methods for understanding three-dimensional supersonic flows. Journal of Visualization, 23(5), 851-862. doi: 10.1007/s12650-020-00662-x
11. Vaisakh, S., & Muruganandam, T. M. (2021). Alternate Schlieren Techniques in High-Speed Flow Visualization. Proceedings of the National Aerospace Propulsion Conference, Singapore.
12. **Van Dyke, M., & White, F. M. (1982). An Album of Fluid Motion. Journal of Fluids Engineering, 104(4), 542-543. doi: 10.1115/1.3241909** (HIGHLY RECOMMENDATION!)

References

Mode Decomposition

13. Chen, K., Zhang, Y., & Zhong, Q. (2019). Wavelet Coherency Structure in Open Channel Flow. Water, 11(8), 1664. doi: 10.3390/w11081664
14. **J. Nathan Kutz, S. L. B., Bingni W. Brunton, and Joshua L. Proctor. (2016). Dynamic Mode Decomposition: Data-Driven Modeling of Complex Systems. doi: 10.1137/1.9781611974508** (This is a book with DMD and POD MATLAB code and examples attached.)
15. Müller, J., Oberleithner, K., Sekimoto, A., Eisfelder, M., Buchner, A.-J., Kitsios, V., Atkinson, C., & Soria, J. (2019). Modal analysis of coherent structures in a self-similar turbulent boundary layer with adverse pressure gradient. doi:
16. Rodríguez-López, E., Carter, D. W., & Ganapathisubramani, B. (2021). Dynamic mode decomposition-based reconstructions for fluid–structure interactions: An application to membrane wings. Journal of Fluids and Structures, 104, 103315. doi: 10.1016/j.jfluidstructs.2021.103315
17. **Rowley, C. W., & Dawson, S. T. M. (2017). Model Reduction for Flow Analysis and Control. Annual Review of Fluid Mechanics, 49(1), 387-417. doi: 10.1146/annurev-fluid-010816-060042**
18. Schmid, P. J. (2010). Dynamic mode decomposition of numerical and experimental data. Journal of Fluid Mechanics, 656, 5-28. doi: 10.1017/S0022112010001217
19. Taira, K., Brunton, S. L., Dawson, S. T. M., Rowley, C. W., Colonius, T., McKeon, B. J., Schmidt, O. T., Gordeyev, S., Theofilis, V., & Ukeiley, L. S. (2017). Modal Analysis of Fluid Flows: An Overview. AIAA Journal, 55(12), 4013-4041. doi: 10.2514/1.J056060
20. **Taira, K., Hemati, M. S., Brunton, S. L., Sun, Y., Duraisamy, K., Bagheri, S., Dawson, S. T. M., & Yeh, C.-A. (2020). Modal Analysis of Fluid Flows: Applications and Outlook. AIAA Journal, 58(3), 998-1022. doi: 10.2514/1.J058462**
21. Tu, J. H., Rowley, C. W., Luchtenburg, D. M., Brunton, S. L., & Kutz, J. N. (2014). On dynamic mode decomposition: Theory and applications. Journal of Computational Dynamics, 1(2), 391-421. doi: 10.3934/jcd.2014.1.391
22. Zhang, Q., Liu, Y., & Wang, S. (2014). The identification of coherent structures using proper orthogonal decomposition and dynamic mode decomposition. Journal of Fluids and Structures, 49, 53-72. doi: 10.1016/j.jfluidstructs.2014.04.002

NUS National University of Singapore | College of Design and Engineering

Thank you for your listening !

Questions?

Huanxia WEI & Hao HU

16. November 2023